EFFICIENCY OF LIQUID FLAT-PLATE SOLAR ENERGY COLLECTOR WITH SOLAR TRACKING SYSTEM

by

Marija CHEKEROVSKA[a] and Risto Vasil FILKOSKI[b*]

[a] Faculty of Mechanical Engineering, University "Goce Delchev", Shtip, Republic of Macedonia
[b] Faculty of Mechanical Engineering, University „Sts Cyril and Methodius",
Skopje, Republic of Macedonia

Original scientific paper
DOI: 10.2298/TSCI150427099C

An extensive testing programme is performed on a solar collector experimental set-up, installed on a location in town of Shtip (Republic of Macedonia), latitude 41^o 45' and longitude 22^o 12', in order to investigate the effect of the Sun tracking system implementation on the collector efficiency. The set-up consists of two flat-plate solar collectors, one with a fixed surface tilted at 30^o towards the south, and the other one equipped with dual-axis rotation system. The study includes development of a 3-D mathematical model of the collectors system and a numerical simulation programme, based on the computational fluid dynamics approach. The main aim of the mathematical modelling is to provide information on conduction, convection, and radiation heat transfer, so as to simulate the heat transfer performances and the energy capture capabilities of the fixed and moving collectors in various operating modes. The feasibility of the proposed method was confirmed by experimental verification, showing significant increase of the daily energy capture by the moving collector, compared to the immobile collector unit. The comparative analysis demonstrates a good agreement between the experimental and numerically predicted results at different running conditions, which is a proof that the presented computational fluid dynamics modelling approach can be used for further investigations of different solar collectors configurations and flow schemes.

Key words: *renewable energy, solar thermal collector, energy efficiency, heat transfer, computational fluid dynamics*

Introduction

As a result of the growing energy needs in the households, agriculture, industry and other sectors, especially in the developing countries, the demand for energy has increased remarkably in recent years. One of the negative consequences is the rapid growth in the level of harmful emissions, including greenhouse gas emissions and the increase in fuel prices, which are the main driving forces behind efforts to utilize renewable energy sources (RES) more effectively. However, as the most RES depend on the climate daily and seasonal variations, their effective use usually requires complex design, planning and control optimization methods [1].

A simple and most direct application of the solar energy is its conversion into heat, which is also one of the ways the residential and other sectors can lessen their share in electricity consumption. Wider use of solar thermal collectors can reduce the annual expenses for

* Corresponding author; e-mail: risto.filkoski@mf.edu.mk

domestic water heating by significant share; in some regions, due to the specific climate conditions, reaching as much as 40-50%. Solar water heater performance and its geographic variation have been analyzed for 147 different sites in all European countries [2].

Due to the favorable climate conditions in the Southern European countries, the possibilities of implementation of solar collectors for conversion of solar energy into heat and/or electricity were a subject of research efforts in many works, such as [3, 4], demonstrating significant potential for fossil fuels and electricity replacement. A specific approach, using energy and exergy methods, is implemented for analysis of solar assisted heat pump space heating system in the work of Atmaca and Kocak [5]. The case study is applied and simulation results are given for the conditions in Antalya city, Turkey. An experimental study of evacuated tube solar water heater system with two collector types, water-in-glass and heat-pipe, is performed by Chow *et al.* [6]. Performance tests were carried out in the city of Hong Kong, under almost identical boundary conditions by placing the two collectors side-by-side.

An 1-D mathematical model for simulating transient processes that occur in liquid flat-plate solar collectors is presented by Zima and Dziewa [7], where the main properties, variables and the boundary conditions are considered as time-dependent. Ayoub in [8] investigates methods of harvesting solar radiation with a flat-plate collector in cloudy-sky conditions, in order to optimize the energy capture of the system, proposing an improved method for irradiance optimization by using a controlled tracking system. The optical performance of solar panels, equipped with a sun-tracking system adjusted at three fixed positions on a daily basis, is theoretically investigated by Zhong *et al.* [9], based on a proposed mathematical method and monthly horizontal radiation. A mathematical procedure for estimation of the annual collectible radiation on fixed and tracked panels is suggested by Li *et al.* [10]. Compared to fixed south-facing solar panels inclined at an optimal tilt-angle, the increase in the annual solar gain due to sun tracking is calculated in the areas with abundant solar resources and in the areas with poor solar resources.

The study of Catarius [11] is carried out in order to investigate the performance of dual-axis solar tracking system. According to the report, in the conditions the research was performed, the use of dual-axis tracking system increases the annual energy gain by around 48%, compared to an immobile solar panel and by around 36%, compared to a collector with single-axis tracking system.

A comprehensive literature review on different modelling approaches of solar collector systems is given by Saleh [12]. Also, a 1-D mathematical model for simulating the transient processes that occur in liquid flat-plate solar collectors is proposed in the same work [12]. The model considers time-dependent thermo-physical properties and heat transfer coefficients.

Simulation of the heat transfer phenomena in flat-plate solar collectors using commercial CFD codes is presented in [13], by considering the mixed heat transfer modes of conduction, convection, and radiation between tube surface, glass cover, side walls, and insulating base of the collector, and their results achieved good agreement with test data. The work of Bakić *et al.* [14] deals with the numerical simulation of the air flow around the arrays of flat plate collectors and determination of the flow field, which should provide a basis for estimating a convective heat losses. The results obtained with the numerical simulation of flow around collectors were used as boundary conditions in modelling of thermal-hydraulic processes inside the solar collector. Wang and Wu [15] have proposed a discrete numerical model to calculate the flow and temperature distribution in order to analyze the performance of flat-plate solar collector with Z-arranged collector arrays, in which the flows are parallel in the dividing and combining manifolds.

The work of Kessentini *et al.* [16] deals with an experimental and numerical research of a flat plate collector prototype with plastic transparent insulation and low-cost overheating protection. The numerical model is based on the resolution of the different components of the collector by means of a modular object-oriented platform. Experimental and theoretical investigation of the flow and temperature distribution in a solar collector panel with an absorber consisting of horizontally inclined fins is presented in the work of Fan *et al.* [17]. The flow and heat transfer in the collector panel are studied numerically, by means of CFD technique, as well as experimentally. The 1-D model of a flat-plate collector has been developed and experimentally validated in the work of Rodriguez-Hidalgo *et al.* [18]. The model consists of calculation of the thermal resistances and thermal heat capacitances in order to determine the collector heat loss and the thermal inertia.

Rahbar and Esfahani [19] have estimated the hourly yield of a single-slope solar collector by use of a 2-D CFD simulation model. The obtained results are in a good agreement with the results of well-known models, they show that there is an optimum length in which the productivity is maximized. A detailed numerical model of a flat-plate solar collector is developed by Cadafalch [20]. It is noticed by the author that the flow and the heat transfer through the collector are essentially 1-D. The developed model is an extension of the Duffie and Beckman model [21] and it is verified by an experiment data conducted on single and double glazed collectors under steady-state conditions.

The present work deals with experimental and mathematical analysis of two flat-plate solar collectors, one static and one moving equipped with a sun tracking system, which could be easily applied to other devices without changing or redesigning the collector's shape. The main objectives of the research are: to derive a mathematical model that portrays the operation of a flat-plate solar collector under transient conditions, to calculate the flow and temperature distribution for any cross-section at any certain time, to analyze the overall performance of flat-plate solar collector and to experimentally verify the proposed mathematical model. Also, one of the aims of the work is to demonstrate the potential of the use of CFD simulations, together with experiments, in order to obtain a more detailed insight into the flow and transport processes in facilities for solar energy utilization.

Theoretical background

Two main components of the solar energy collector system, which are required in order to have a functional solar energy heat generator are a collector and a storage unit, the last one needed due to the solar energy non-constant nature. A typical flat-plate solar collector consists of an absorber in an insulated box, including a pipeline system filled with working fluid, transparent cover sheets (glazing) and other components. The absorber is usually made of a metal sheet of high thermal conductivity, such as copper or aluminum, with integrated or attached tubes. Its surface is coated with a special selective material to maximize radiant energy absorption, while minimizing emission. The insulated box reduces heat losses from the back and sides of the collector. The cover sheets allow sunlight to pass through to the absorber, but insulate the space above the absorber to prevent cool air from flowing into this space. However, the glass also reflects a small part of the sunlight, which therefore does not reach the absorber.

For a detailed analysis of flow and heat transfer, it is necessary to set-up a 3-D model, which considers time-dependent change of variables and includes conservation equations for mass, momentum and energy, solar ray tracing, and thermal radiation modelling. Because of the nature of the solar energy, the working conditions of the solar collector regarding the heat transfer and fluid flow are unavoidably transient and non-uniform.

A comprehensive modelling of a flat-plate solar collector should consider an incompressible, predominantly laminar fluid flow problem, which includes heat transfer in fluid and solid regions, as well as solar radiation to semi-transparent and other surfaces. The flow is mostly steady and possesses laminar flow characteristics, as the fluid flow velocity through the manifolds and vertical pipes is low. Under steady-state conditions, the overall energy balance is defined as:

Heat energy delivered by the collector = Heat energy absorbed by the plate and the pipes – – Heat losses to the surroundings

In the case of a solar collector, the heat transfer includes conduction, convection, and radiation within fluid and solid regions and the process should necessarily be analyzed as transient phenomenon. An overall energy balance of a flat-plate solar collector is illustrated in fig. 1 [22, 23], indicating the distribution of the incident solar energy into useful energy gain, thermal losses and optical losses.

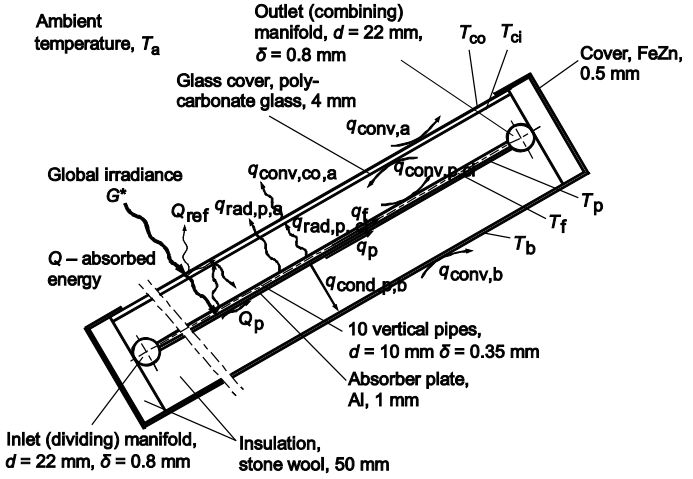

Figure 1. A schematic representation of an energy balance of a flat-plate solar collector [22, 23]
conv – convection,
cond – conduction,
rad – radiation,
a – ambient,
c – cover (glass),
co – cover outer,
ci – cover inner,
p – absorber plate,
f – fluid,
b – back (tin cover)

The input parameters of the model are detailed geometrical and physical properties of the collector, climatic, and operation parameters. Basic outputs of the model are usable thermal energy gain Q_u [W] and collector efficiency. The useful gain from the collector Q_u is defined:

$$Q_u = A_c[S - U_L(T_{pm} - T_a)] \tag{1}$$

where A_c [m^2] is the gross area of the collector glass cover, S [Wm^{-2}] – the insolation on the plane of the absorber, U_L [Wm^{-2}K^{-2}] – the collector overall heat loss coefficient, T_{pm} [K] – the mean fluid temperature in the absorber, and T_a [K] – the ambient temperature.

The collector installation thermal efficiency is defined as the ratio of the useful thermal energy gain Q_u to the incident solar energy on the plane of the absorber, over a specified time period.

Methodology of the research

Experimental work

The experimental set-up considered in this study was located in the town of Shtip, latitude 41^o 45’ and longitude 22^o 12’, fig. 2 [24]. The system, schematically presented in fig.

3, consists of: a moving collector equipped with a two-axis tracking device (a programmable chronological tracker is used to control the motion of the moving collector), static collector, horizontal water tank, circulating pumps, non-return valves, flow-meters, three-way valves, expansion vessel, manometers, air-vent devices, pressure-relief valves, drain valves, cold water entrance, automatics, temperature sensors, solar irradiation (heat flux) sensor, *etc.*

Figure 2. Experimental set-up and a segment of the tracking system: electric drive (a); gear spindle (b); auxiliary mechanism (c)

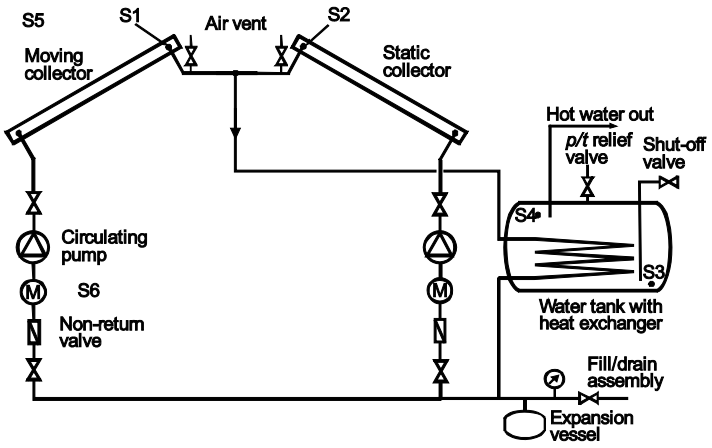

Figure 3. A schematic diagram of an experimental set-up; *S1 – temperature sensor of the moving collector, S2 – temperature sensor of the static collector, S3 – temperature sensor of the cold water in the tank, S4 – temperature sensor of the hot water in the tank, S5 – solar irradiation sensor, S6 – flow meter for the moving and static collectors*

The experimental set-up has two hydraulic circles, the first one composed of a collector (static or moving one), heat exchanger in a horizontal water tank and an associated equipment and the other one composed of a horizontal tank of 150 liters and heated water consumers. Working fluid in the primary circle is a 50:50% water and propylene glycol mixture by weight. Each collector is a flat-plate, consisting of two manifolds, dividing and combining one, and 10 Cu tubes in a Z-arrangement. The main technical parameters of the collectors are given in tab. 1 [24].

Using the measured parameters, the collector thermal efficiency is calculated:

$$\eta_c = \frac{m_f c_{p,f} (T_{f,\text{out}} - T_{f,\text{in}})}{GA_c} \tag{2}$$

where m_f [kgs^{-1}] is the working fluid mass flow rate, $c_{p,f}$ [Jkg^{-1}K^{-1}] – the average specific heat capacity of the working fluid, $T_{f,\text{out}}$ [K] – the working fluid outlet temperature,

$T_{f,\text{in}}$ [K] – the working fluid inlet temperature, G [Wm^{-2}] – the total normal incident radiation, and A_c [m^2] – the area of the collector aperture.

Table 1. Main technical parameters of the solar collector [24]

Description	Specification
Collector annotation	Eко Mag 2
Collector body	Aluminum
Dimensions, in mm	1500 × 970 × 81
Fluid content (water and propylene glycol)	1.76 liters
Vertical pipes: number, material, dimensions	10, Cu, 10.0/0.35 mm/mm
Manifolds (headers): number, material, dimensions	2, Cu, 22.0/0.8 mm/mm
Absorber plate	Aluminum, selective color
Thermal insulation	Mineral wool, 50 mm
Transparent (glass) cover	Polycarbonate glass, 4 mm
Maximum temperature	165 °C
Weight	18 kg

Numerical model set-up and simulations

The flat-plate solar collector geometry considers the transient properties of its different zones. The numerical domain for the mathematical model comprises all functionally important parts of the collector, presented with their real geometry: manifolds (distributing and combining), vertical pipes, working fluid, transparent (glass) cover, absorber plate, air region, and thermal insulation. The back and sides metal cover is also included in the model.

The geometry was created using Gambit pre-processor [25]. The basic geometry of the collector pipe system used in the research, with the main dimensions, the outline of the computational domain and the mesh generated for calculations, are presented in fig. 4 [23]. The numerical grid consists of 791033 volume cells and 171743 computational nodes. The grid independence was tested and verified using three different grids, in order to ensure that the grid resolution would not have a notable impact on the results: (1) 632800 volume cells, (2) 791033 volume cells (with 171743 nodes), and (3) 949300 volume cells [23]. Since the grid refinement changed the results by less than 0.5%, which was previously decided as criteria, it was concluded that the influence of eventual further refinement would be negligible and, therefore, the mesh (2) was taken as appropriate for computation.

The numerical simulations were carried out using steady-state implicit pressure based solver [25]. The governing partial differential equations for mass and momentum are solved for the steady incompressible flow. The velocity-pressure coupling has been effected through the SIMPLEC algorithm. Second order upwind scheme was chosen for the solution scheme. The turbulence is covered with the RNG k-ε turbulence model and standard wall functions for the near-wall treatment. The considered case includes CFD modelling of solar irradiation, modes of mixed convection and radiation heat transfer between the tubes surfaces, glass cover, absorber, and side walls of the collector. It also covers mixed convection in the circulating water/propylene glycol mixture inside the tubes and conduction between the absorber plate, the tubes material, the insulation region, and the collector cover.

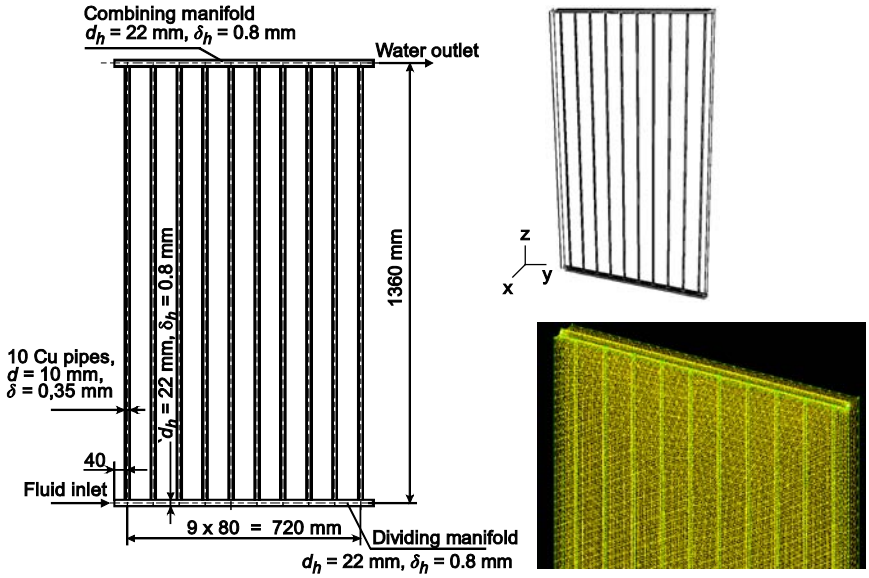

Figure 4. The collector pipeline system geometry, the outline of the numerical domain, and the numerical mesh [23]

Heat transfer, thermal radiation, and solar load modelling, boundary conditions, and operating parameters

The selection of the most appropriate thermal radiation model in certain conditions depends on various factors, and in the case of solar collector modelling it becomes even more complex due to the necessity to include solar load model. The discrete transfer radiation model has been already proved as an efficient radiant transfer method in solar energy collector applications [26]. In the present study, it was decided to correlate the experimental results with a mathematical model that incorporates the discrete ordinates (DO) radiation method, due to the opportunity of applying a solar load directly to the DO model [25]. The DO radiation method considers the radiate transfer equation (RTE) in the direction **s** as a field equation:

$$\frac{\mathrm{d}I(\vec{\mathrm{r}},\vec{\mathrm{s}})}{\mathrm{d}s}+(a+s_s)I(\vec{\mathrm{r}},\vec{\mathrm{s}})=an^2\frac{\sigma_0 T^4}{\pi}+\frac{\sigma_s}{4\pi}\int_0^{4\pi} I(\vec{\mathrm{r}},\vec{\mathrm{s}}')\Phi(\vec{\mathrm{s}}\,\vec{\mathrm{s}}')\mathrm{d}\omega' \tag{3}$$

where $I(\vec{\mathrm{r}},\vec{\mathrm{s}})$ [Wm^{-2}srad^{-2}] is the spectral intensity, λ – the wavelength, a [m^{-1}] – the spectral absorption coefficient, $\vec{\mathrm{r}}$ [–] – the location vector, $\vec{\mathrm{s}}$ [–] – the direction vector (defined as $\vec{\mathrm{s}}=\mu\vec{i}+\eta\vec{j}+\xi\vec{k}$), $\vec{\mathrm{s}}'$ [–] – the vector of scattering direction, σ_s [m^{-1}] – the scattering coefficient at wavelength λ, σ_0 [Wm^{-2}K^{-4}] – the Stefan-Boltzmann constant, $\sigma_0 = 5{,}672\cdot10^{-8}$, ω' [–] – the solid angle, and Φ – the phase function, which represents the probability that a ray with frequency v' from the direction $\vec{\mathrm{s}}$ in a finite discrete solid angle dω' will veer in the direction $\vec{\mathrm{s}}'$ inside the angle dω, with frequency v.

The DO radiation model solves the RTE for a finite number of discrete solid angles, each associated with a vector direction $\vec{\mathrm{s}}$, fixed in the Cartesian system. The fineness of the angular discretization can be changed accordingly and the DO model solves as many transport equations as there are directions **s**. In this case, the so-called S6 approximation was applied,

corresponding to 48 flux approximations [26]. This approach gives sufficiently reasonable results for the amount of the numerical work. The higher-order approximations, such as the S8, with 80 flux approximations, require considerably more numerical effort. Appropriate boundary conditions were imposed on the numerical domain, for the inlet of the working fluid a *velocity inlet* boundary condition is specified and for the outlet, an *outflow* condition is specified.

The values of the properties of the collector materials for the CFD analysis purposes are presented in tab. 2 [24]. Polynomial interpolation formulae are used in the calculations for the thermo-physical properties of the water/propylene glycol mixture and for the air, given in tabs. 3 and 4 [23].

Table 2. Properties of the materials used in the experimental research [24]

Property, unit	Absorber plate, Al	Water pipes, Cu	Insulation (mineral wool)	Transparent cover (glass)
Density, [kgm^{-3}]	2720	8800	60-200	2230
Specific heat capacity, [Jkg^{-1}K^{-1}]	875	4200	1000	750
Thermal conductivity, [Wm^{-1}K^{-1}]	210	380	0.04 (at 20 °C)	1.05
Transmissivity	0	0	0	0.84
Emissivity (IR emittance)	0.95	0.95	–	0.1
Solar absorbance	0.9	0.9	–	–

Table 3. Properties of the water/propylene glycol mixture *T* [K] [23]

Density, [kgm^{-3}]	$\rho = 978.2 + 0.973T - 0.003T^2 + 1.0\cdot10^{-6}T^3$
Dynamic viscosity, [kgm^{-1}s^{-1}]	$\mu = 1.4274 - 0.016T + 7\cdot10^{-5}T^2 - 1\cdot10^{-7}T^3 + 9\cdot10^{-11}T^4$
Specific heat capacity, [Jkg^{-1}K^{-1}]	$c_{p} = 3901 - 2.674T + 0.0058T^2 + 5\cdot10^{-8}T^3$
Thermal conductivity, [Wm^{-1}K^{-1}]	$\lambda = 0.2674 - 0.0002T$

Table 4. Properties of the air *T* [K] [23]

Density, [kgm^{-3}]	$\rho = 2.829 - 0.0084T + 0{,}00001T^2 - 5\cdot10^{-9}T^3$
Dynamic viscosity, [kgm^{-1}s^{-1}]	$\mu = 5\cdot10^{-8} + 4\cdot10^{-10}T$
Specific heat capacity, [Jkg^{-1}K^{-1}]	$c_{p} = 1014.7 - 0.0005T + 0.0001T^2$
Thermal conductivity, [Wm^{-1}K^{-1}]	$\lambda = 0.0228 + 8\cdot10^{-5}T$

Results

There is a complex matrix of measurement results from the experimental research, conducted in the spring 2010, as well as a plentiful of results arising from the CFD simulations. In this section, just a small share of the available experimental and CFD modelling results are presented, with aim to give an overview of the provided study. The experimentally obtained increase in the solar heat gain due to the use of a two-axes tracking system is shown in fig. 5, compared to the energy gain of a fixed south-facing solar collector, inclined at an optimal tilt-angle in a given day. The tracking collector showed a better performance with an in-

crease in the collected energy of above 20% over the considered period (March-April), compared to the fixed one. Temperature contours of the air gap and the working fluid on a level 0.68 m from the central axis of the inlet dividing manifold are given in fig. 6, obtained with the RNG k-ε turbulence model, using the standard values of the model constants [25].

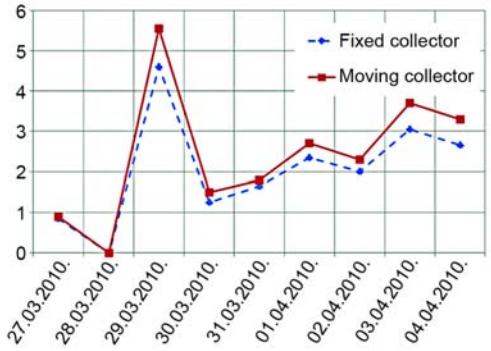

Figure 5. Thermal energy [kWh] produced by solar collectors in a given day

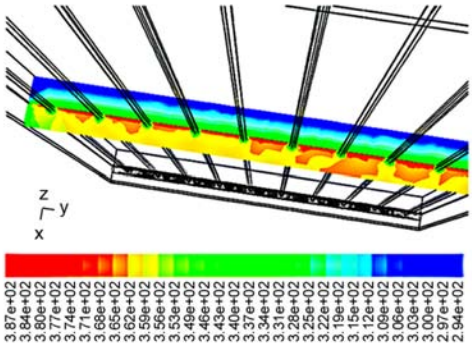

Figure 6. Temperature profiles in a horizontal intersection *(for color image see journal web-site)*

A comparative analysis between the experimental data and the numerical simulation results is a basis for optimization of the design and the operation mode of the collector. In order to accomplish this, measurements are conducted in different meteorological conditions, while keeping the main collector parameters fixed, which means that the solar radiation flux for the simulation module is varied. Charts regarding five days of collectors operation are shown in figs. 7 to 11, indicating the total solar radiation change, as well as the change of the measured and numerically simulated temperatures of the working fluid (propylene glycol/water mixture) at the collector exit, over time. It can be seen from the charts how the variations of the solar radiation daily change affect the temperature change of the collectors' working fluid. For instance, while the weather conditions on March 20 and April 4 were characterised by smooth change, on March 16 variations of the solar radiation occurred on hourly basis and March 25 was characterised with sharp decline of the radiation between 11.00 and 12.00 hours. In these figures S3 presents the change of the cold water temperature in the tank (see fig. 3).

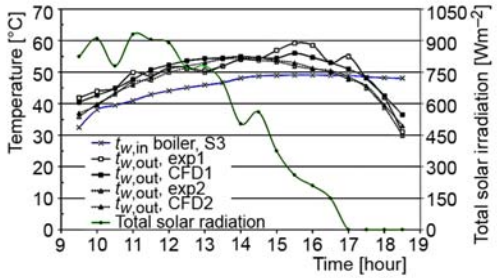

Figure 7. Solar radiation and working fluid temperature change, a comparison between the experimental and CFD results on 16.03.2010

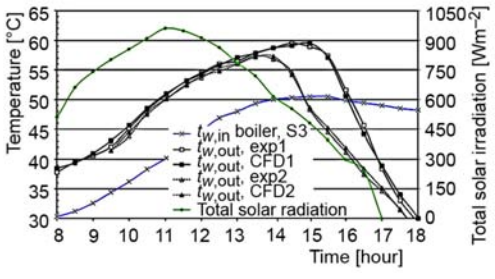

Figure 8. Solar radiation and working fluid temperature change, a comparison between the experimental and CFD results on 20.03.2010

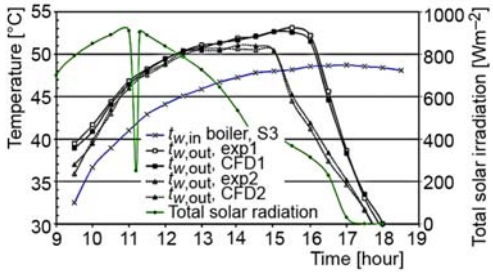

Figure 9. Solar radiation and working fluid temperature change, a comparison between the experimental and CFD results on 25.03.2010

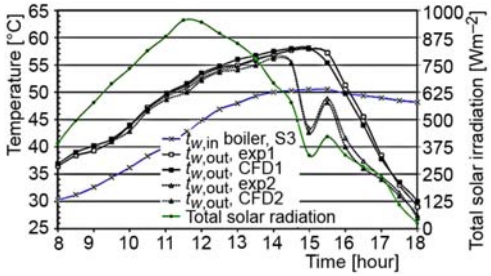

Figure 10. Solar radiation and working fluid temperature change, a comparison between the experimental and CFD results on 01.04.2010

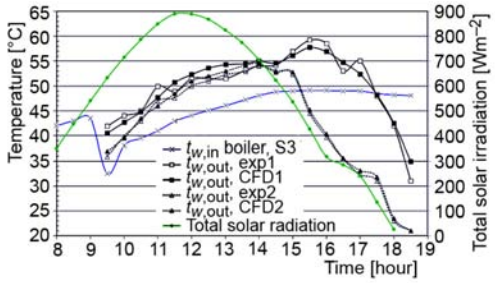

Figure 11. Solar radiation and working fluid temperature change, a comparison between the experimental and CFD results on 04.04.2010

The measured total solar radiation on the experimental facility spot is also given in figs. 7 to 11, in order to correlate the change of its value with the collector working fluid temperature change. From the presented diagrams, it is obvious that the frequent (fig. 7) or quick but sharp lows (fig. 10) in solar irradiation have consequent impact on the change of the working fluid temperature. In general, the temperature change of the working fluid is quite well predicted by the numerical simulations.

The temperature rise coefficient, C_T, is defined by the equation:

$$C_T = \frac{T_f - T_{f,\text{in}}}{T_{f,\text{out}} - T_{f,\text{in}}} \tag{4}$$

where T_f is the actual working fluid temperature, $T_{f,\text{in}}$ – the fluid inlet temperature, and $T_{f,\text{out}}$ – fluid outlet temperature. According to the provided numerical simulations as for the conditions on 4 April 2010, 13.00 CET, the temperature rise coefficient at working fluid velocity of 0,01 m/s is presented in fig. 12, where the non-dimensional flow length is defined as the ratio between the distance from the beginning of the pipe to the specific (measurement and/or modelling) point and the total length of the tube. The temperature difference band between the absorber plate and the fluid increases at larger velocities, due to higher thermal resistance between the absorber plate and the fluid. The change of the working fluid temperature versus velocity, $w_{f,\text{i}}$ in certain operating conditions, according to the CFD simulations, as for the conditions on 4 April 2010, 13:00 CET, is given in fig. 13. In this diagram, the annotation means: $w_{f,1}$ = 0.0001 m/s, $w_{f,2}$ = 0.0005 m/s, $w_{f,3}$ = 0,001 m/s, $w_{f,4}$ = 0,005 m/s, and $w_{f,5}$ = 0,01 m/s. The working fluid in the absorber tubes gets differentially heated with very high temperature rise for lower mass flow rate (and consequent lower velocity), followed by almost constant heat transfer when the absorber and fluid temperatures become closer.

Conclusions

The comparative experimental and numerical research of the fixed and solar tracking collector systems' performances has led to several conclusions. The collector equipped with

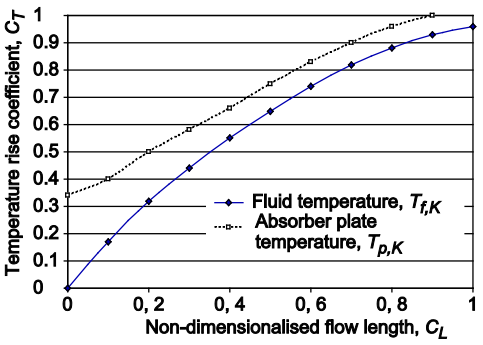

Figure 12. Temperature rise coefficient of absorber plate and fluid, corresponding to w_f = 0.01 m/s on 4 April 2010, 13:00 CET

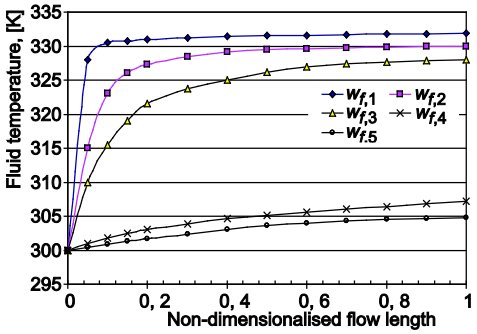

Figure 13. Fluid temperature *vs.* velocity, corresponding to 4 April 2010, 13:00 CET

solar tracking system, constructed for the purpose of this work, has shown a clear benefit over immobile (static) collector system, which is particularly obvious in the afternoon hours. Due to the limitations of the experimental research, in order to provide a complete analysis at different operating conditions, a comprehensive CFD modelling and simulation was undertaken. The analysis shows that there is a good agreement between the experimental and numerically predicted values for different running conditions and flow rates. It can be noticed that the CFD model results are closer to the experimental data in the case of the static collector. The modelling approach can be successfully applied for investigation of other configurations of solar receivers, such as air solar collectors and solar concentrators with various configurations.

References

[1] Banos, R., *et al.*, Optimization Methods Applied to Renewable and Sustainable Energy: A Review, *Renewable and Sustainable Energy Reviews, 15* (2011), 4, pp. 1753-1766

[2] Yohanis, Y. G., *et al.*, Geographic Variation of Solar Water Heater Performance in Europe, *Proc. IMechE, Part A: J. Power and Energy, 220* (2005), 4, pp. 395-407

[3] Stefanović, V. P., Bojić, M. Lj., Development and Investigation of Solar Collectors for Conversion of Solar Radiation into Heat and/or Electricity, *Thermal Science, 10* (2006), 4 (Suppl.), pp. S177-S187

[4] Ledesma J. T., *et al.*, Numerical Simulation of the Solar Thermal Energy Storage System for Domestic Hot Water Supply Located in South Spain, *Thermal Science, 17* (2013), 2, pp. 431-442

[5] Atmaca, I., Kocak S., Theoretical Energy and Exergy Analyses of Solar Assisted Heat Pump Space Heating System, *Thermal Science, 18* (2014), Suppl. 2, pp. S417-S427

[6] Chow, T. T., *et al.*, Experimental Study of Evacuated-Tube Solar Water Heaters in Hong Kong, *Proc. IMechE Part A: J. Power and Energy, 226* (2011), 4, pp. 447-461

[7] Zima, W., Dziewa, P., Modelling of Liquid Flat-Plate Solar Collector Operation in Transient States, *Proc. IMechE Part A: J. Power and Energy, 225* (2010), 1, pp. 53-62

[8] Ayoub, H., Improving the Energy Capture of Solar Collectors (For Cloudy Regions by Using Controlled Tracking System), M. Sc. thesis, University of Strathclyde, Department of Mechanical and Aerospace Engineering, Glasgow, UK, 2012

[9] Zhong, H., *et al.*, Optical Performance of Inclined South–North Axis Three-Positions Tracked Solar Panels, *Energy, 36* (2011), 2, pp. 1171-1179

[10] Li, Z., *et al.*, Optical Performance of Inclined South-North Single-Axis Tracked Solar Panels, *Energy, 35* (2010), 6, pp. 2511-2516

[11] Catarius, A., Azimuth-Altitude Dual Axis Solar Tracker, A Master Qualifying Project, Worcester Polytechnic Institute, Worcester, Mass., USA, 2010

[12] Saleh, A., Modeling of Flat-Plate Solar Collector Operation in Transient States, M. Sc. thesis, Purdue University, Fort Wayne, Ind., USA, 2012
[13] Selmi, M., *et al*., Validation of CFD Simulation for Flat Plate Solar Energy Collector, *Renewable Energy, 33* (2008), 3, pp. 383-387
[14] Bakić, V. V., *et al.*, Numerical Simulation of the Air Flow around the Arrays of Solar Collectors, *Thermal Science, 15* (2011), 2, pp. 457-465
[15] Wang, X., Wu, L., Analysis and Performance of Flat-Plate Solar Collector Arrays, *Solar energy, 45* (1990), 2, pp. 71-78
[16] Kessentini, H., *et al.*, Development of Flat Plate Collector with Plastic Transparent Insulation and Low-Cost Overheating Protection System, *Applied Energy, 133* (2014), Nov., pp. 206-223
[17] Fan, J., *et al.*, Flow Distribution in a Solar Collector Panel with Horizontally Inclined Absorber Strips, *Solar Energy, 81* (2007), 12, pp. 1501-1511
[18] Rodriguez-Hidalgo, M. C., *et al*., Flat Plate Thermal Solar Collector Efficiency: Transient Behavior under Working Conditions. Part I: Model Description and Experimental Validation, *Applied Thermal Engineering, 31* (2011), 14-15, pp. 2394-2404
[19] Rahbar, N., Esfahani, J. A., Productivity Estimation of a Single-Slope Solar Still: Theoretical and Numerical Analysis, *Energy, 49* (2013), Jan., pp. 289-297
[20] Cadafalch, J., A Detailed Numerical Model for Flat-Plate Solar Thermal Devices, *Solar Energy, 83* (2009), 12, pp. 2157-2164
[21] Duffie, J. A., Beckman, W. A., *Solar Engineering of Thermal Processes*, 2nd ed., Wiley Interscience, New York, N. Y., USA, 1991
[22] Hochenauer, C., Solar Thermal Flat-Plate Collectors – 1D and 3D Simulation, FH Oberosterreich, Muhlkreis, Austria, http://www.technolog.at/files/ WS_B3_Pruefung_thermischer_Sonnen kollektoren _ Teil_1.pdf
[23] Filkoski, R. V., Chekerovska, M., Experimental and Numerical Study of a Flat-Plate Solar Energy Collector Performance, *Proceedings on CD* (Ed. Olabi, A. G.), 7th International Conference on Sustainable Energy & Environmental Protection (SEEP), Dubai, UAE, 2014, Vol. 1, paper S01076
[24] Shumanska, M., A Contribution to Defining the Impact of the Tracking of a Hot Water Flat Plate Solar Collector on its Efficiency, M. Sc. thesis, University "Sts Cyril and Methodius", Faculty of Mechanical Engineering, Skopje, Republic of Macedonia, 2010
[25] ***, Fluent Inc., Fluent 6.2 User's Guide, Lebanon NH 03766, USA, 2005
[26] Karanth, K. V., *et al*., Numerical Simulation of a Solar Flat Plate Collector Using Discrete Transfer Radiation Model (DTRM) – A CFD Approach, *Proceedings* (Eds.: S. I. Ao, L., Gelman, D. W., Hukins, A., Hunter, A. M., Korsunsky), World Congress on Engineering 2011 (WCE 2011), London, 2011, Vol. III, pp. 2355-2360

Paper submitted: April 27, 2015
Paper revised: June 30, 2015
Paper accepted: July 1, 2015